Electronic structure of rare-earth pnictides

A. G. Petukhov
Department of Physics, Case Western Reserve University, Cleveland, Ohio 44106-7079
*and Physics Department, South Dakota School of Mines and Technology, Rapid City, South Dakota 57701-3995**

W. R. L. Lambrecht and B. Segall
Department of Physics, Case Western Reserve University, Cleveland, Ohio 44106-7079
(Received 5 June 1995)

The results of first-principles calculations of the electronic band structures, equilibrium lattice constants, cohesive energies, bulk moduli, and magnetic moments are presented for the rare-earth pnictides with the rocksalt structure and chemical formula *R-V*, where $R=$Gd, Er, and the group-*V* elements N, P, and As. The linear-muffin-tin-orbital method was used in the atomic sphere approximation. The $4f$ states were treated as localized corelike states with fixed spin occupancies. Justifications for this procedure are presented. The systems were studied with the $4f$ spins on all rare-earth ions aligned (ferromagentic phase) and with the spins randomly oriented (paramagentic phase). Within the local spin-density approximation, all systems studied were found to be semimetallic with a hole section of the Fermi surface near Γ and electron section near X. The nitrides, however, have a nearly zero band-gap overlap. We estimated quasiparticle self-energy corrections using an approach previously used for semiconductors. With these corrections, GdN is found to be a semiconductor in the paramagnetic phase and a semimetal in the ferromagnetic phase. ErN, on the other hand, is found to be a semiconductor in both phases. All systems correspond to a trivalent state of the rare-earth element and are characterized by ionic bonding. The results for the lattice constants and the qualitative conclusion about the semimetallic nature are in agreement with experimental data and with the previous calculations for Gd-pnictides. For ErAs, the calculated magnetic exchange splittings, electron and hole concentrations, Fermi-surface cross-sectional areas, and cyclotron masses are in satisfactory agreement with the available Shubnikov–de Haas data on $Er_xSc_{1-x}As$ when account is taken of the differences due to the presence of Sc and of the self-energy corrections to the local-density approximation.

I. INTRODUCTION

The rare-earth pnictides (i.e., group-*V* compounds), which we shall denote *R-V*, form an interesting family of materials, because of the great variety of their magnetic and electrical properties,[1] despite their common simple crystal structure, the rocksalt structure. An interesting aspect of these compounds is the occurence of localized strongly correlated $4f$ electrons, the treatment of which presents a challenge to band-structure theory. The strong exchange coupling between the localized rare-earth $4f$ spins and the valence and conduction electrons in these materials (which are either semimetals or semiconductors) also leads to interesting magnetic properties. For example, the *R*-As and *R-P* compounds have antiferromagnetic ground states, while the corresponding *R-N* compounds are ferromagnets.[2] The spin ordering vector is along the unusual $\langle 111\rangle$ direction. The Néel and Curie temperatures of these materials are extremely low (a few K). These properties are rather intriguing. While they are perhaps not of great use for usual magnetic applications, the exchange coupling of the valence bands to the $4f$'s offers the possibility of modifying the electronic properties of the *R-V* compounds by an external magnetic field. This might in turn be used to magnetically tune *R-V*/semiconductor interface properties, e.g., in spin superlattices. Previous work on spin superlattices has focused on dilute magnetic impurties in semiconductors, such as $Zn_{1-x}Mn_xSe$/ZnSe.[3] *R-V* compounds offer the prospect of achieving a much larger concentration of local magnetic moments in such systems and hence the observation of large enhancements of the Zeeman effects on the valence and conduction bands.

Recently, the interest in these materials has sharply increased by the demonstration that they can be grown epitaxially on semiconductors.[4–7] This opens the way to the development of electronic devices, such as metal base transistors.[5] Important progress towards this goals was achieved by Palmstrøm *et al.*,[4] by demonstrating heteroepitaxial growth of rare-earth monoarsenide $Er_xSc_{1-x}As$ on GaAs and vice-versa. Allen *et al.*[8] explored the band structure of these thin epitaxial films of $Er_xSc_{1-x}As$ buried in GaAs by measurements of the Hall resistance, transverse magnetoresistance, and Shubnikov–De Haas (SdH) oscillations. This study showed that $Er_xSc_{1-x}As$ is a semimetal with an electron and a hole concentration of $(3.1\pm0.1)\times10^{20}$ cm^{-3} and has large exhange splittings induced by the $4f$ open shell. Further details of the Fermi surface were obtained by subsequent SdH studies at higher magnetic fields by Bogaerts *et al.*[9–11]

The first band-structure investigation from first-principles of the rare-earth group-*V* compounds was carried out by Hasegawa and Yanase (HY) (Ref. 12) and was concerned with the Gd monopnictides (GdSb, GdAs, GdP, and GdN). Later, calculations were also reported on CeSb,[13] DyBi, and DyP.[14] Closely related are studies of the *IIIb-V* compounds, such as LaSb, LaBi,[15] and ScN.[16,17] In the absence of results on Er-V compounds, the first interpretations of the experimental investigations of $Er_xSc_{1-x}As$ (Refs. 8–10) were largely based

directly on HY's work on the Gd-V compounds[12] and subsequent tight-binding calculations by Xia *et al.*,[18] which were parametrized by means HY's results. This is obviously not completely satisfactory. While one expects a qualitative similarity between the band structures of Gd and Er compounds, there must be quantitative differences, especially regarding the exchange splittings. Also, HY's calculations did not include spin-polarization effects and used the $X\alpha$ potential instead of employing local spin-density (LSD) functional theory. In a previous paper,[19] we focused on the analysis of these experiments, using LSD calculated band structures of ErAs and $Er_xSc_{1-x}As$.

Recently, resonant tunneling devices with a thin ErAs layer sandwiched between AlAs barriers embedded in GaAs were fabricated and their behavior in the presence of a magnetic field were studied by Zhang *et al.*[20] A theoretical study of the latter based on our band-structure results will be presented elsewhere.[21]

In this paper, we present a band-structure study of some other R-V compounds: namely, those with $R=$Er, Gd and $V=$As, P, N. A preliminary report on these results was presented in Ref. 22. In the present paper, we describe these results in full. Our reasons for studying the Gd compounds, in addition to those of Er, are that this provides a comparison with the early work of HY,[12] and, in addition, allows us to evaluate the effects of different $4f$ shell filling. One expects larger spin induced effects in Gd than in Er. Our decision to consider a range of pnictides permits us to study the trends with the group-V element. Of particular interest here is the information obtained about the R nitrides. From previous work,[1,12,16] it is not even clear whether these materials are semimetals or semiconductors. One reason for this is the uncertainties on the band gaps in LSD calculations. The comparison with experimental Fermi-surface data in our previous work on ErAs (Ref. 19) allows us to make estimates of the quasiparticle corrections beyond the LSD theory. We, thus, are also able to make more reliable estimates of the gap corrections for the nitrides. In this connection, we note, as was pointed out in Monnier *et al.*'s[17] study of ScN, that an indirect semiconductor with a sufficiently small gap may undergo a phase transition to a metallic electron-hole liquid ground state.

Finally, there were no previous attempts to calculate the equilibrium properties, such as cohesive energies, equilibrium lattice constants, and bulk moduli for this family of materials. The results presented here remedy this situation for the R-V compounds considered.

Additional first-principles total energy calculations will be required to establish the relative stability of different magnetic phases of these materials and are planned for the near future. In the present paper, we limit ourselves to the paramagnetic and ferromagnetic phases. The latter can also be thought of as the saturated limit of the paramagnetic state in a magnetic field.

The paper is organized as follows: Sec. II describes our computational method with special emphasis on our treatment of $4f$ states and localized versus itinerant magnetic moments. In Sec. III, we present some test calculations for ErAs and GdAs, justifying our treatment of the $4f$ electrons as corelike states rather than bandlike states. We then describe our main results in Sec. IV. Section IV A describes our total energy results. Section IV B presents the band structures without spin polarization and describes the nature of the bonding. Section IV C describes the spin-polarized band structures and exchange splittings at the Fermi level. Section IV D presents results on the induced magnetic moments. Section IV E describes the calculated Fermi surfaces. A comparison with experimental data for $Er_xSc_{1-x}As$ is given. While this part has already been presented in Ref. 19, it is briefly summarized here in order to make the paper self-contained. In addition, we briefly address some aspects of these data involving spin-orbit coupling corrections, an issue not addressed in our previous work. Section IV F gives calculated effective masses. The discussion, Sec. V, provides estimates for the quasiparticle corrections (Sec.V A), which leads to improved values for the gaps of the nitrides and returns to the question of the interactions with the $4f$ electrons in Sec. V B. Finally, Sec. VI summarizes our conclusions and draws attention to some of the most interesting predictions of the present work.

II. COMPUTATIONAL METHOD

Except for the special treatment of the $4f$ electrons discussed below, the general framework within which the calculations are performed is the density functional theory[23] in the local (spin-) density approximation [L(S)DA].[24] The linear-muffin-tin-orbital (LMTO) method[25] is used in the atomic sphere approximation (ASA), including both the combined correction term and the muffin-tin or Ewald correction.[26] As usual for non-closed-packed lattices, empty spheres[27] were introduced in the appropriate interstices: here centered at $(a/4)(1,1,1)$ and $(a/4)(3,3,3)$. The atomic and empty spheres were all chosen to be of equal size, thus making the underlying sphere packing the same as in the bcc structure for which the ASA is known to be accurate.

The calculations were performed scalar relativistically. The Brillouin zone integrations were performed with the tetrahedron method[28] on a regular mesh of 1000 points in the Brillouin zone of the rocksalt lattice. These were found to be sufficient to provide well-converged results.

Because of the strongly correlated nature of $4f$ electrons, they cannot be adequately described within the standard LSDA framework, which is essentially a one-electron theory. A sounder conceptual starting point is provided by the periodic Anderson Hamiltonian.[29] Here, it describes a narrow $4f$ band with strong Coulomb correlations, which can hybridize with broadbands (e.g., Er $5d$, As $4p$) in which explicit Coulomb correlations are neglected (or, more precisely in our case, are treated at the LSDA level in an effective one-electron approximation. A first approximation to this Hamiltonian consists of neglecting the hopping between $4f$ orbitals. It is then reduced to the Anderson ''impurity'' Hamiltonian. A further approximation neglects the coupling between the narrow and the broadbands. In this approximation, the charge density of the $4f$ states becomes essentially independent of the Bloch-related boundary conditions at the Wigner-Seitz sphere, which can be replaced by ''atomic'' boundary conditions. Clearly, this works because of the very localized nature of the $4f$ electrons, which is a result of the high centrifugal ''barrier'' $l(l+1)/r^2$ for the $4f$ electrons. Thus, in spite of the fact that their energetic position may

overlap the broadbands of the system, these levels form a very narrow resonance. In this treatment, the dominant on-site Coulomb terms can be included easily. Total energy calculations with different occupations of the $4f$ level (treated as an impurity by either a Green's function or supercell technique) can be used to obtain the effective on-site Coulomb interaction U.[30] From such calculations — or, equivalently, from Slater's transition state approach[31] — one may also obtain the binding energy of the $4f$ level with respect to the Fermi level. We have not actually carried out such calculations for the present materials, but can anticipate what the result would be from studies on similar systems. The important self-interaction correction for the ground state occupation $4f^n$ will effectively lead to a $4f$ band position well below the Fermi level, even though this $4f$ band is not completely filled. U is sufficiently large that the state $4f^{n+1}$ with an additional $4f$ electron lies above the Fermi level. Estimates of U for our systems can be obtained from a combination of photoemission and inverse photoemission spectra for the pure rare-earth metals.[32,33] The basic features of the occupied and empty $4f$ level position, with respect to the bands, are also excellently discussed by Herbst *et al.*[45] Since it is clear that in the present case the rare-earth element is trivalent (we will, in fact, prove it to be by varying the $4f$ occupation), the ground state corresponds to $4f^{11}$ for Er and $4f^7$ for Gd. Within our corelike treatment of the $4f$ states, this completely specifies the $4f$ charge density, even though we did not really attempt to calculate the actual binding energies of the $4f$ levels. That this approach is accurate for the rest of the band structure will be shown by its success in describing total energy ground state properties as well as detailed agreement with magnetotransport measurements.

We now turn to the magnetic effects. We know from the atomiclike multiplet splittings,[1] of the $4f$ states in Er^{+3} and Gd^{+3} ions, that Hund's first rule is satisfied. (Again, our LSDA calculations for the atoms also find this rule to hold.) We can thus choose fixed $4f$ spin-up and spin-down occupation numbers corresponding to the maximal total spin configuration. The existence of the localized magnetic moments resulting from the $4f$ spins in the R-V compounds has been well established[8] even up to fairly elevated temperatures (e.g., well above the Néel temperature in ErAs). The magnetism in these materials is thus a combination of localized magnetic moments from the open $4f$ shell and induced itinerant magnetic moments in the valence bands. Above the Néel or Curie temperatures, these moments remain well established and almost constant (for all temperatures of intrest here), but point in random directions. In fact, a reasonably strong magnetic field can align them, as described by the classical Brillouin theory of paramagnets.[8]

In this context, we need to discuss briefly the meaning of our calculations with or without spin polarization. The low Néel temperature ($T_N = 4.5 \pm 0.25$ K in ErAs) (Ref. 8) indicates that the energetic difference between the antiferromagnetic and paramagnetic phases is small. This is consistent with the existence of the moments above T_N mentioned above. Clearly, intra-atomic $4f$ spin polarization will make a substantial contribution to the total energy both in the (anti-) ferromagnetic and paramagnetic states. We hence include the spin-polarization contribution of the $4f$ states to the total energy in both phases. The fully spin-polarized $4f$ electrons in the paramagnetic phase produce a strong spin-dependent random potential for band electrons. The situation is quite similar to that in a disordered alloy. The electronic structure of such a ''spin alloy'' could, for example, be calculated by means of the coherent potential approximation.[34] From the point of view of the alloy model, a non-spin-polarized LDA calculation may be viewed as corresponding to the virtual crystal approximation.

The spin-polarized calculations, on the other hand, may be thought of as representing either a ferromagnetic phase or the saturation limit of the paramagnetic phase in a magnetic field. In the case of the arsenides and phosphides, the latter interpretation is more relevant, because the actual magnetic structure at low temperature is antiferromagnetic. The induced magnetic moments in the valence bands will differ from those in the ferromagnetic state considered here. In fact, anticipating the results of Sec. IV A, we note that in the ferromagnetic phase, the spins on the R-$5d$ are parallel to the $4f$ spin, while opposite spins are also induced on the As. Since we know from experiment[2] that the spins in the antiferromagnetic phase order along $\langle 111 \rangle$, a direction along which R planes and As planes alternate, the net spin on the As atom in that case can be expected to be zero by symmetry, because it lies between an up-spin R and a down-spin R plane, so that the opposite exchange couplings must cancel each other.

It should be noted that the treatment of rare-earth $4f$ electrons has been somewhat controversial. While the early work[12,35] tended to follow our present approach of treating $4f$'s as core states, later work emphasized the need for including the band character of $4f$ electrons.[36–38] Effectively, the present treatment of the $4f$ electrons as open shell corelike states is equivalent to the *constrained* local spin-density functional approach of Dederichs *et al.*[40] It is also closely related to that used by Hasegawa and Yanase,[12] who used a frozen core treatment. Brooks *et al.*[35] used a similar approach in their treatment of rare-earth-transitional-metal compounds, although they used slightly different boundary conditions for the $4f$ states at the Wigner-Seitz sphere. The papers by Brooks *et al.*[35] and Ahuja *et al.*[39] provide excellent discussions of this controversy with ample references to the previous literature.

In order to further justify our procedure, we have also performed a few test calculations, in which the band character of the $4f$'s is taken into account. As will be shown in Sec. III, a straightforward LSDA band treatment for the $4f$'s in ErAs and GdAs leads to very different and definitely poorer results than the approach described above and the one followed for the remainder of the paper. This is obvious because the band treatment must lead to a narrow $4f$ band at the Fermi level. In addition, we will show that it strongly perturbs the rest of the band structure. Our corelike treatment, on the other hand, is expected to be closer to the actual situation in which a set of narrow occupied $4f$ levels, several eV below the Fermi level and a narrow set of unoccupied $4f$ states several eV above it only have a minor effect on bands near the Fermi level. From the above calculations, we obtain an estimate of the effective $4f$ band width resulting from the $4f$ hopping and hybridization to the broadbands, i.e., the terms we neglected in the Anderson Hamiltonian. Together with estimates of U, these terms can be used to gauge their

effect on the Fermi surface. In fact, we will use these estimates to argue that the effect is negligible and hence justifies our procedure.

It is thus clear, as far as the quasiparticle excitation spectra are concerned, that narrow bands like $4f$ cannot be treated adequately in a LSDA single-particle band picture. Treating them as semilocalized core states is a convenient and reasonable way to remove them from the electronic spectrum near the Fermi energy on which we are focusing in the present work. Of course, for a study of the spectral features directly involving the $4f$ states, such as, e.g., photoemission, additional calculations are required. For example, their binding energies could be calculated by means of the transition state procedure mentioned above. Alternative treatments such as LDA$+U$ have been proposed by others.[41,13] Essentially, such a treatment corresponds to a Hartree-Fock treatment of the average $4f$ electron configuration with a screened effective U. A Hartree-Fock like treatment for $4f$ electrons was also proposed by Bylander and Kleinman.[42] The essential feature of these models is that the energy functional is orbital dependent rather than only density dependent. For the present purpose, which is mainly to describe the band structure relevant for transport (i.e., the states near the Fermi level), we do not need this more elaborate treatment of the $4f$ electrons.

As far as ground state properties are concerned, the charge density associated with the $4f$ electrons appears to be sufficiently well described without taking into account their band dispersion. That description is also more convenient, since it avoids problems with reaching self-consistency related to the occurence of very narrow $4f$ bands at the Fermi level in a single-particle band picture.

Because of the high ionicity of the present compounds, the rare-earth $6p$ like states were on average found to make only a small contribution to the valence bands of interest. On the other hand, our fairly small Wigner-Seitz radii for the rare-earth ions (due to the use of empty spheres) meant that the $5p$ semicore electronic states were not completely adequately described with atomic boundary conditions. They were hence included in the basis set as band states instead of the $6p$ like bands. This was found to be important for the total energy properties, especially under compressive stress.

III. TEST CALCULATIONS

In this section, we describe some test calculations of ErAs and GdAs strictly within LSDA, i.e., treating the $4f$ states as bands. By comparison to the results described in Secs. IV B, IV C, which will be shown to be in good agreement with experiment, we argue that a strict band treatment for the $4f$ states is totally inadequate.

Figure 1 shows the results of a self-consistent calculation for ErAs including the $4f$ states as bands and neglecting spin polarization. As expected, a narrow $4f$ band is present at the Fermi level. The width of this band is about 0.2 eV. Comparison with Fig. 2(c) shows that this band has a strong perturbing effect on the other bands. Specifically, the mainly As 4p derived band, which has a ''valence-band maximum'' at Γ_{15} forms bonding and antibonding states with the $4f$ band, which lie, respectively, 0.5 eV below and 1.7 eV above the Fermi level. This leads to a very heavy mass for the bonding

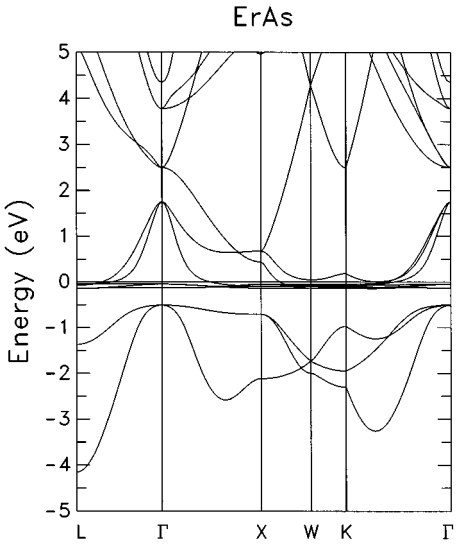

FIG. 1. Band structure of ErAs in which Er $4f$ states are treated as bands without taking into account the strong Coulomb interactions. The $4f$'s are seen to strongly perturb the band structure compared to that in Fig. 4(c).

state below the Fermi level. The Er $5d$ derived band, which crosses the As 4p band along Δ, remains completely above the Fermi level instead of dipping below it at X. The pure LDA band structure is thus incompatible with the observed semimetallic nature of ErAs. Here, we ignore the narrow $4f$ band, which, one might argue, would not contribute to the normal electronic transport, because of its narrowness.

In ErAs, even if we include spin polarization, a partially filled $4f$ band is expected at the Fermi level and hence similar strong perturbation of the remaining bands is obtained. In GdAs, where the $4f$ shell is exactly half filled, one might

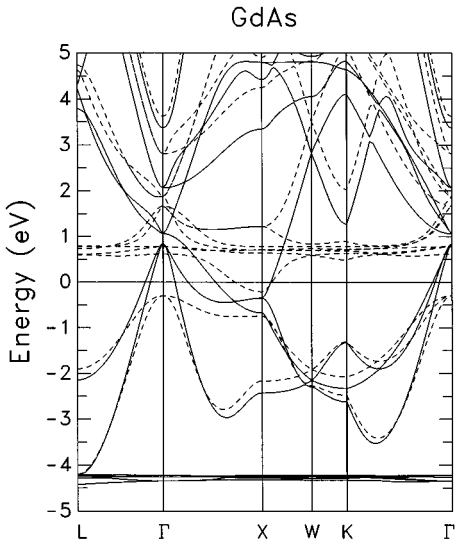

FIG. 2. Spin-polarized band structure of GdAs (dashed lines are the minority spin bands), in which Gd $4f$ states are treated as bands without taking into account the strong Coulomb interactions. The $4f$'s are seen to strongly perturb the minority spin bands, while the majority spin bands are in fair agreement with the band structure of Fig. 4(c).-

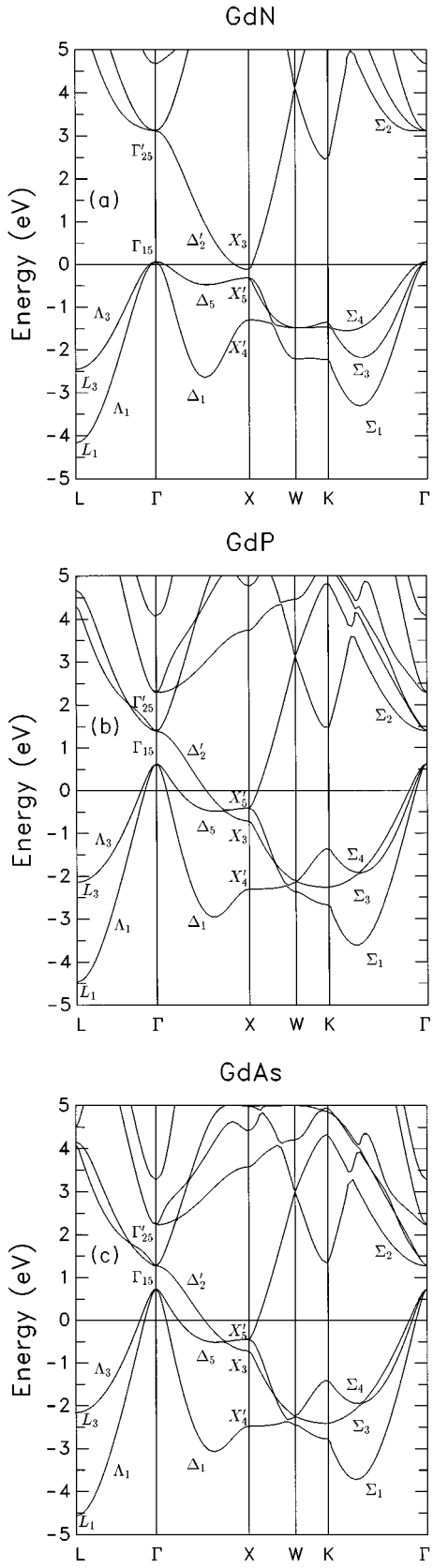

FIG. 3. Non-spin-polarized electronic band structure of gadolinium pnictides: (a) GdN, (b) GdP, and (c) GdAs.

expect that the LSDA treatment would be better. Figure 3 shows that this is the case for the majority spin bands, but not for the minority spin bands. Indeed, the occupied $4f\uparrow$ band lies at about 4.3 eV below the Fermi level and the spin-up As $4p$-derived and Er $5d$-derived bands are similar in character to their counterparts in Fig. 4(c) (see Sec. IV B). However, the $4f\downarrow$ lies less than 1 eV away from the Fermi surface and shows strong perturbation effects on the remaining spin-down bands similar to that for ErAs.

Clearly, a pure band treatment of the $4f$ levels is not adequate. We will return to the question of the $4f$ band effects on the Fermi surface in the discussion in Sec. V B.

IV. RESULTS

A. Cohesive and elastic properties

As explained in Sec. II, we carried out both non-spin-polarized LDA and spin-polarized LSDA band structure and total energy calculations with fixed numbers of $4f$ spin-up and spin-down electrons, assuming that $4f$ spins of different rare-earth ions are aligned ferromagnetically in the fully spin-polarized state. The calculations were performed for different values of the rocksalt lattice constant a and the Rose *et al.*[43] equation of state was then fitted to the $E(a)$ curves in order to determine the equilibrium a, bulk modulus B, and its pressure derivative $B'=dB/dp$. Variation of the total number of $4f$ electrons shows that the energetically stable configurations of the rare-earth ions correspond to the charge state R^{3+}, i.e., to $n_{4f}=7$ in the Gd compounds and $n_{4f}=11$ in the Er compounds.

In Table I, we present the results of our total energy calculations. As can be seen from this table, the calculated equilibrium lattice constants are in rather good agreement with experimental data. They are, as is usual for the LDA, slightly lower than the experimental values. We are currently not aware of any data on the bulk moduli or their pressure derivatives. The values obtained appear reasonable in comparison with those of known semiconductor and transition-metal pnictides.

As mentioned above, the valence electron (excluding $4f$) contribution to the total energy $E_{\rm tot}^{P,\rm LDA}$ obtained from the non-spin-polarized LDA calculations can be considered as that of the paramagnetic phase, while the total energy of fully spin-polarized state $E_{\rm tot}^{F,\rm LSDA}$ with $n_{4f\uparrow}-n_{4f\downarrow}=7$ in the Gd compounds and $n_{4f\uparrow}-n_{4f\downarrow}=3$ in the Er compounds can be associated either with the ferromagnetic phase or with the paramagnetic phase in the presence of an external magnetic field sufficiently strong to produce complete spin alignment. (Note that the energy of interaction with the external filed is not included explicitly.)

The results of LSDA calculations for free atoms show that in accordance with Hund's rule the ground state of both Gd and Er atoms corresponds to the fully polarized atomic configuration with maximal total spin, i.e., to the $4f^7 5d^1 6s^2 (S=4)$ for Gd and $4f^{11} 5d^1 6s^2$ $(S=2)$ for Er. The corresponding cohesive energies are defined as the difference between $E_{\rm tot}$ and the energy of free R and X atoms in their fully spin-polarized state. For the solid's paramagnetic phase, we add a correction for the intra-atomic $4f$ spin polarization energy, which is not included in our band-structure calculation of the non-spin-polarized LDA total energy. The energy of $4f$ spin polarization can be extracted from a separate atomic calculation in which we consider the hypothetical atomic configuration with fully polarized $4f$ shell and non-

TABLE I. Equilibrium lattice constants, cohesive energies, and bulk moduli.

Compound	a (Å), theor.	a (Å), exp.[a]	$E_{\rm coh}^{P,\rm LDA}$ [b]	$E_{\rm coh}^{F,\rm LSDA}$ [c]	B (GPa)	B'
GdN	4.977	4.999	5.874	5.956	188.47	4.4
GdP	5.704	5.729	5.280	5.321	94.16	4.0
GdAs	5.843	5.854	4.951	4.989	86.04	4.1
ErN	4.789	4.839	4.447	4.452	220.25	4.3
ErP	5.557	5.595	3.552	3.553	102.95	3.8
ErAs	5.700	5.732	3.172	3.174	93.70	4.1

[a]Reference 1.

[b]Cohesive energy (eV/atom) for the paramagnetic phase (including the $4f$ spin-polarization energy E_{4f}, but no spin polarization of the valence electrons), with respect to neutral atoms in their fully spin-polarized LSDA ground state. Zero point motion is not included.

[c]Cohesive energy (eV/atom) of the ferromagnetic phase (fully spin polarized).

polarized $5d$ shell, i.e., $n_{5d\uparrow}=n_{5d\downarrow}=1/2$ and $S=S_{\max}-1/2$. The difference between the total energy of this configuration and the total energy of the non-spin-polarized configuration with the same total populations of particular shells and $S=0$ gives the energy of intra-atomic spin polarization of $4f$ electrons:

$$E_{4f}=E_{\rm tot}(S_{\max}-1/2)-E_{\rm tot}(0). \tag{1}$$

The value of E_{4f} obtained for Gd was 8.96 eV and for Er was 1.74 eV. These values are then added as a correction to our non-spin-polarized total energy calculaton for the solid because, as mentioned in Sec. II, the $4f$ moments are assumed to persist in the paramagnetic state, but are disordered so that they do not induce a net spin polarization in the rest of the bands.

The cohesive energies of the paramagnetic and ferromagnetic phases of R-V compounds are listed in the Table I. The closeness of these energies for a given compound confirms the fact that the spin polarization energy of the band electrons represents a very small contribution to the cohesive energy in comparison with E_{4f} and is consistent with the small Néel temperature. The fact that these (small) energy differences are significantly larger in the Gd compounds than the Er compounds reflects the larger $4f$ moments in the former. We note that within the precision of our numerical procedure the theoretical values of the lattice constants are the same in both the paramagnetic an ferromagnetic phases. An adequate study of the phase transition between the paramagnetic and (anti-) ferromagnetic phases would require a more rigorous treatment of the paramagnetic phase (e.g., including fluctuation effects) and would require the determination of the actual preferred magnetic ordering (antiferromagnetic, ferromagentic, or other).

B. Non-spin-polarized band structure and nature of the bonding

The non-spin-polarized LDA band structures of Gd-V and Er-V compounds for V=As, P and N are shown in Figs. 3 and 4, respectively. The most striking feature of these results is the remarkable similarity of the bands of the corresponding Gd and Er compounds. These differ only in minor details, which are almost undiscernable on the scale of the figures. Another important general feature is that the bands of the phosphides and arsenides are very similar, while those for the nitrides differ significantly. While the former are clearly semimetals with a hole section of the Fermi surface near Γ and an electron section near X, the nitrides have almost a zero gap overlap. The results for Gd-V compounds are in good agreement with those of Hasegawa and Yanase.[12]

The lowest valence band is essentially pnictogen (i.e., group-V element) s like. It is not shown in the figures, because we want to provide better resolution for the more important higher lying bands. It lies in the range -13 to -11 eV for the nitrides, -10.5 to -8.5 eV for the phosphides and -11 to -9.5 eV for the arsenides. The next set of three are pnictogen p-like bonding with R $5d$. The next five bands are mainly R $5d$ like, which are antibonding with pnictogen p. At Γ, these split into a threefold t_{2g} state and a doubly degenerate e_g state. The fact that the lowest R $5d$-derived band, which along Γ-X in the x direction is essentially d_{yz} like, dips below the mainly pnictogen-p-like band (crossing it near X) is responsible for the semimetallic character of the material. Finally, the next higher conduction-band state at Γ is $6s$ like. As emphasized in Sec. II, here, we are not attempting to calculate the $4f$ band positions. Since they are decoupled from the valence bands by our treating them as corelike states, they do not appear in the band structures of Figs. 3 and 4.

Despite our decoupling of the $4f$ electrons, we noted in Sec. IV A above that we obtain the correct $4f$ occupation, that corresponding to a trivalent state of the rare-earth ion, by minimizing the total energy with respect to $4f$ occupation. Basically, this is explained by the fact that allows for the most optimal filling of the three upper pnictogen-p-like valence bands. Thus, although the systems are semimetallic, the bonding is essentially ionic with the R valence charge being transferred to the pnictogen. In contrast to the free atoms situations in which the $6s$ state is occupied, the mainly $6s$ derived bands in the solid are high up in energy, because of their antibonding interactions with the anions and consequently do not significantly participate in the bonding. This is consistent with the notion of a strongly ionic limit of the Er^{+3} or Gd^{+3} ions. So, if it were not for the R-$5d$ states, which dip below the valence bands, these materials would be wide-gap insulators.

C. Spin-polarized bands

The spin-polarized LSDA band structures of GdP and ErP are shown in Figs. 5 and 6, respectively. The spin-polarized

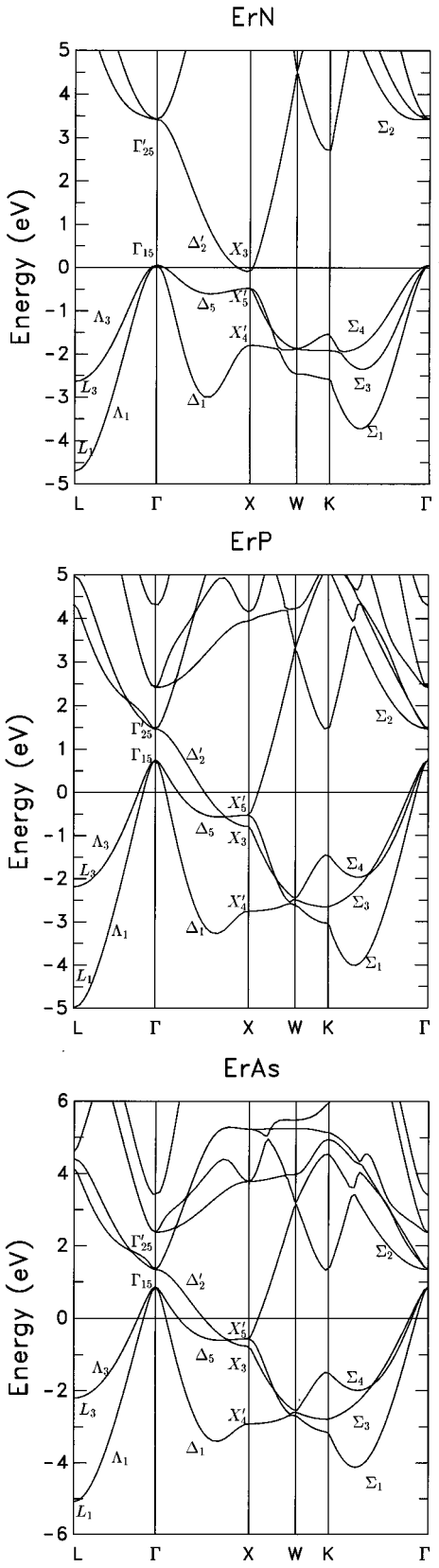

FIG. 4. Non-spin-polarized electronic band structure of erbium pnictides: (a) ErN, (b) ErP, and (c) ErAs.

band structures of the remaining compounds GdAs, GdN, ErAs, and ErN were previously published in Ref. 22 and for ErAs also in Ref. 19. The corresponding densities of states for ErAs and GdAs are presented in Figs. 7 and 8, as an

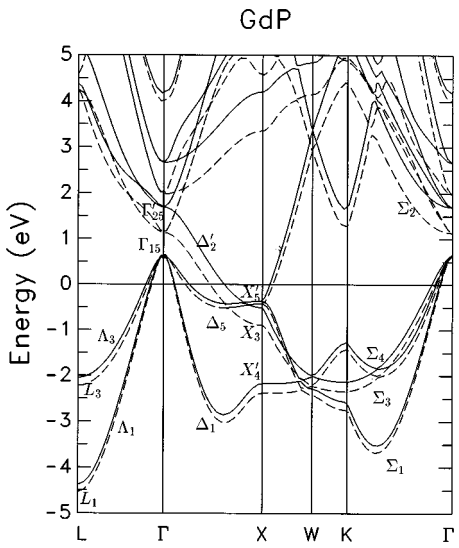

FIG. 5. Spin-polarized electronic band structure of GdP. Dashed lines correspond to the majority spin states (parallel to the $4f$ spins).

example. The principal feature of these results is that the energy bands in Gd-V compounds display much larger exchange splittings than do the corresponding Er-V compounds. Again, this is, of course, due to the larger $4f$ magnetic moment in Gd, which has $S=7/2$ rather than in Er, which has $S=3/2$.

It is interesting to note, that GdN turns out to be semimetallic for spin-down electrons, but has a finite band gap for spin-up electrons (by convention, we chose the direction of the $4f$ spins as ''down''). Further inspection of these results shows that the induced magnetism in the compounds considered cannot be described with a simple rigid shift model, i.e., the splitting of the spin-up and spin-down bands strongly depends on the particular band state. This leads not only to splittings of several peaks in the densities of states, but also

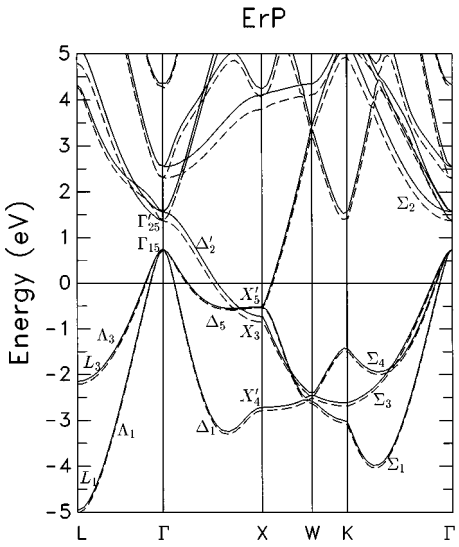

FIG. 6. Spin-polarized electronic band structure of ErP. Dashed lines correspond to the majority spin states (parallel to the $4f$ spins).

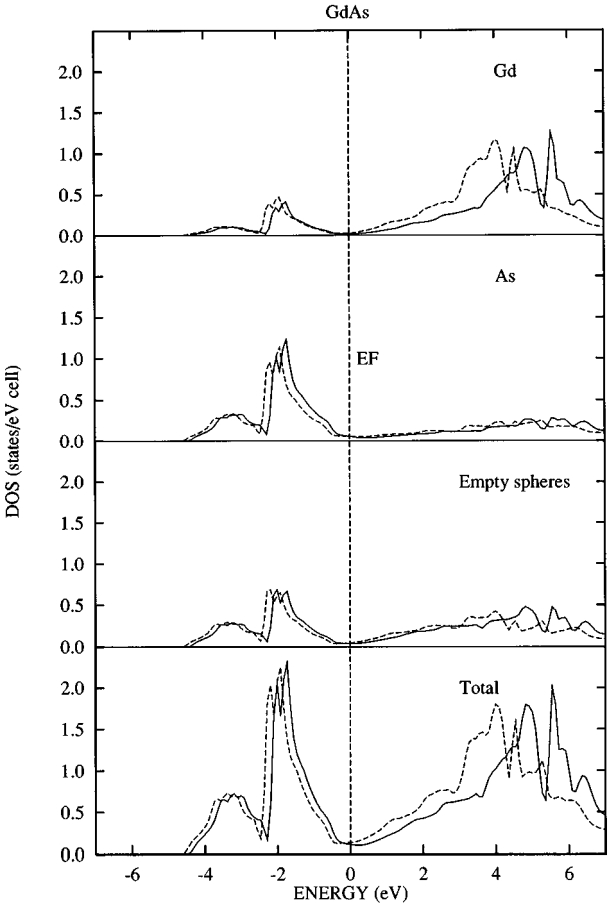

FIG. 7. Local densities of minority spin (solid lines) and majority spin (dashed lines) states in GdAs.

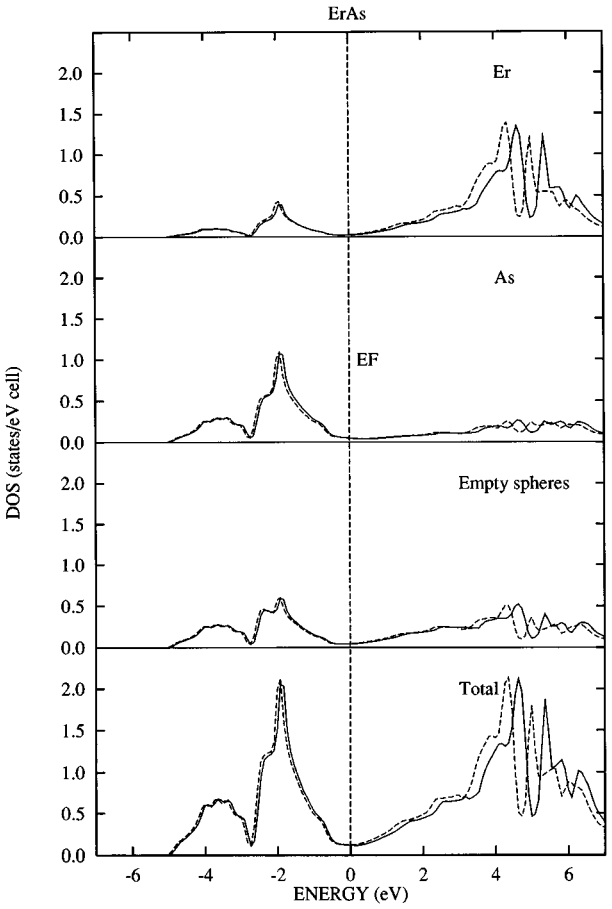

FIG. 8. Local densities of minority spin (solid lines) and majority spin (dashed lines) states in ErAs.

to redistributions in their intensities. Since the upper valence bands are formed mostly by the p states of the pnictogen and the lower conduction bands are formed mostly by the $R\ 5d$, the latter display much stronger exchange splitting.

For the same reason, there is a strong anisotropy of the exchange splitting for conduction electrons near the Fermi surface. The exhange splittings $\Delta_{\rm xc}^{e\perp}$ along X-W and $\Delta_{\rm xc}^{e\parallel}$ along Γ-X are presented in Table II. The reason for this anisotropy is that the conduction band, which crosses the Fermi level in the Γ-X direction, is formed mainly by $R\ 5d$ states, while a share of these states in the perpendicular direction is much smaller. In this table, we also give the much smaller exchange splitting for the holes.

Experimental information on the exchange splittings at the Fermi level is available from Allen *et al.*'s[8] SdH measurements. These were carried out on quasi-two-dimensional (100) layers of $Er_xSc_{1-x}As$, with the magnetic field parallel to (100). They observed beatings in the SdH spectra, due to the different (but nearly equal) areas of extremal orbits for spin-up and spin-down electrons in the plane perpendicular to the magnetic field, and extracted a value of the $\Delta_{\rm xc}^{e\perp}$ in the range 55–91 meV by normalizing their values for two samples of different Er concentrations to 100% Er. Our calculated value of $\Delta_{\rm xc}^{e\perp}=80$ meV, is in good agreement with their range of values, and in fact, agrees extremely well with the value that these authors quote for their sample B, which yielded 81 ± 10 meV after normalization to 100% Er.

A direct experimental value for the longitudinal electron exchange splitting of the Δ_2' energy band is not available. It is implicitly involved in the exchange splitting of the SdH frequencies of the ''longitudinal'' ellipsoids measured by Bogaerts *et al.*,[9] discussed below in Sec. IV E. The experimental value for this splitting in $Er_xSc_{1-x}As$ is 136–170 T (depending on whether we use our peak assignment or the original one of Bogaerts *et al.*[9]) Our calculation appears to overestimate this splitting with a value of 208 T.

We note that the electron exchange splittings of the nitride compounds are significantly larger than those for the arsenides and phosphides. This can be explained by the stronger ionicity of the nitrides. The electron bands involved thus have a stronger rare-earth component.

The exchange splitting of the hole bands at the Fermi level is considerably weaker than that of the electrons, but is not entirely negligible. It is only weakly anisotropic, being

TABLE II. Exchange splittings near the Fermi level in meV.

Compound	$\Delta_{\rm xc}^{\rm hh}$	$\Delta_{\rm xc}^{\rm lh}$	$\Delta_{\rm xc}^{e\parallel}$	$\Delta_{\rm xc}^{e\perp}$
GdN	110	90	510	377
GdP	100	70	423	193
GdAs	140	110	439	213
ErN	30	30	182	162
ErP	40	30	147	70
ErAs	50	40	157	80

TABLE III. Decomposition of the total induced spin moment of band electrons μ_{tot} into moments on the rare-earth μ_R and pnictogen μ_V ions, and into moments asociated with the free electrons μ_e and holes μ_h in units of μ_B per unit cell; and the concentration of both spins of free electrons (holes) $n_e(=n_h)$ per unit cell (and, in parentheses in 10^{20} cm^{-3}).

Compound	μ_R	μ_V	μ_e	μ_h	μ_{tot} [a] ;p	$n_e=n_h$
GdN	0.101	−0.119	0.002	−0.002	$<10^{-4}$	0.002 (0.75)
GdP	0.102	−0.089	0.013	0.004	0.017	0.037 (8.0)
GdAs	0.106	−0.083	0.017	0.005	0.022	0.040 (8.0)
ErN	0.032	−0.037	0.001	−0.001	$<10^{-4}$	0.001 (0.4)
ErP	0.033	−0.027	0.005	0.002	0.007	0.041 (9.5)
ErAs	0.036	−0.027	0.006	0.002	0.008	0.042 (9.0)

[a] μ_{tot} also includes a contribution from empty spheres.

slightly larger along the Δ then the Λ direction. The anisotropy is of the order of 10 meV. Also, it is slightly smaller for the light-hole than for the two heavy-hole bands (which are degenerate along the above two symmetry lines.) In Table II, we give an average iostropic value for the heavy and light holes, the precision of which is about 10 meV. Our values for the hole exchange splitting in ErAs (about 50 meV) is in good agreement with those extracted from the resonant tunneling measurements of Brehmer et al.,[20] as discussed in Ref. 21. For the other materials, no data are available.

D. Magnetic moments

The induced spin moments of the band electrons are listed in Table III. In all materials the induced moments on the rare-earth ions and the anions are opposite to each other and nearly cancel. Note that there is also a contribution from the empty spheres. In the nitrides, this cancellation is almost exact when the empty sphere contribution is included. The net ferromagnetism is thus almost completely due to the $4f$ electrons. We note that the induced moments on the rare-earth ions, which comes from the R $5d$ states, are aligned parallel to the $4f$ spins in accordance with Hund's rule.

We also calculated the separate contributions of the electron and hole pockets to the induced magnetic moments by calculating their respective volumes in k space for each spin polarization. Taking the differences between spin-up and spin-down volumes gives us the net contribution to the induced moment, while adding them up gives us the total carrier concentration. These results are given in columns 4, 5, and 7 of Table III. The fact that these moment contributions do not coincide with the rare-earth and pnictogen contributions, respectively, indicates that there is a significant hybridization of these states.

As mentioned in Sec. II the moments obtained here for the As and P compounds correspond to the ferromagnetic phase or the saturation limit of the paramagnetic phase in the presence of a magnetic field. The induced magnetic moments in the antiferromagnetic phase of these compounds will be different. In particular, we expect that the rare-earth moment would be similar in magnitude to the ones obtained here, while the anion moments would be vanishing.

E. Fermi surface

The calculated effective carrier concentration given in Table III is a factor three larger than the experimental value for ErAs.[8] The study of this discrepancy and the related issues of the Fermi-surface volume was the primary subject of our previous detailed study of $Er_xSc_{1-x}As$.[19] It was found that this is primarily an LDA error, which is similar to the gap problem in semiconductors. As in a semiconductor, where the lowest unoccupied band must be shifted up with respect to the valence band, in the present semimetals, the lowest *mostly* unoccupied band, which here is the R $5d$ band, should be shifted up by a self-energy correction. This leads to a reduction of the effective electron concentration. Since in these systems with only closed sections of the Fermi surface, the hole and electron concentrations must equal, the Fermi level must simultaneously shift with respect to the valence bands. Since this is a more or less rigid shift, it does not significanlty affect quantities like the exchange splitting

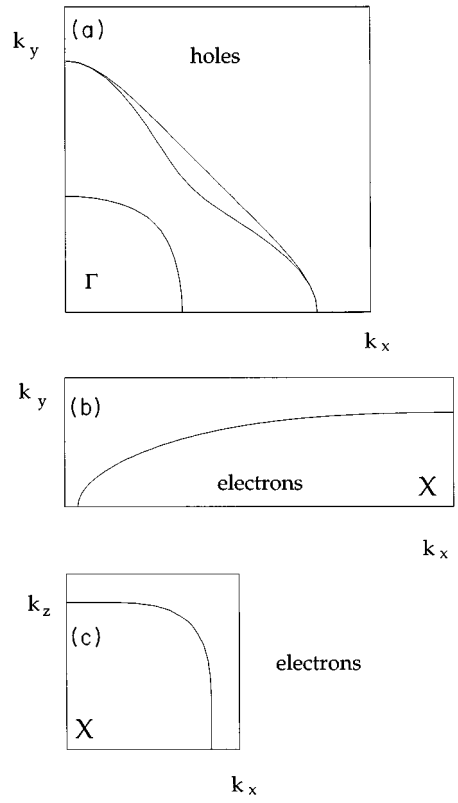

FIG. 9. Cross sections of the Fermi surface of ErAs for (a) holes in the ΓXW plane, (b) electrons in the ΓXW plane, (c) electrons in the WXU plane.

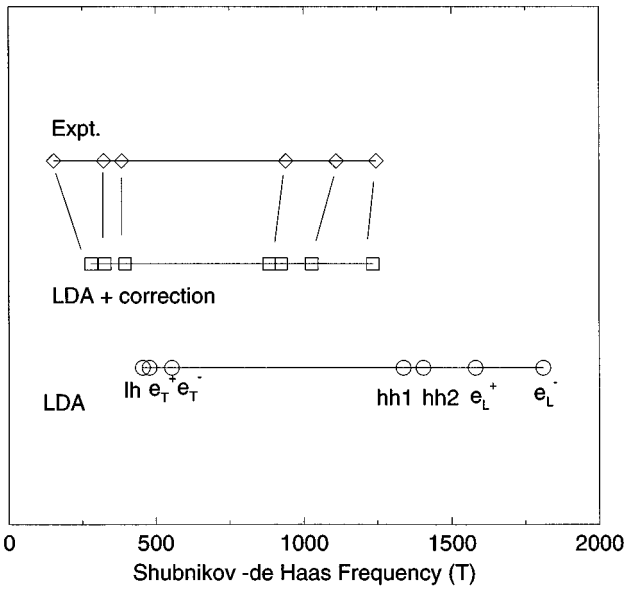

FIG. 10. Comparison of Shubnikov–de Haas frequencies between theory (with and without self-energy shift of Er $5d$) and experiment.

or effective mass parameters very much, but it does affect strongly the overall size of the Fermi surface. Before we further discuss the corrections beyond the LDA, we describe our results for the Fermi surface obtained within LSDA.

The Fermi surfaces have the same topology in all the materials considered. As already mentioned, each consists of closed electron pockets at X and hole pockets at Γ. In Fig. 9, we show the cross section of the hole Fermi surface in the ΓXW plane and the two sections of the electron Fermi surface in the same plane and in the XWU plane. The hole Fermi surfaces consist of three sheets that correspond to the light- and two heavy-hole bands. We note that our present calculations do not include spin-orbit coupling. The effect of spin-orbit coupling would be to split off the band, which here is called the light hole band, and to further increase the splittings between the two heavy-hole bands. For example, their degeneracy along Δ and Λ would be lifted. In semiconductors, these top two bands, denoted here as hh1 and hh2 are referred to as heavy- and light-hole bands. The electron Fermi surface consists of three closed pockets (one at each of the equivalent X points) and contains one sheet, which is ''ellipselike'' in the longitudinal ΓXW and ''squarelike'' in the transverse cross section (XWU). The figure corresponds to the non-spin-polarized calculation. Each of these bands also is split by the exchange splitting in the spin-polarized case. The ellipselike cross section of the Fermi surface is actually rather elongated. One could call it a cigar-shaped Fermi surface rather than an ellipsoidal surface. This is closely related to the band crossing along Δ. In the corrected band structures (see below), the Fermi surface becomes more nearly ellipsoidal.

Direct experimental information on the areas of these various cross sections is available for $Er_xSc_{1-x}As$ from SdH measurements.[8–10] In our previous work,[19] we gave a detailed account of these measurements, which is briefly summarized here in Fig. 10. First of all, our interpretation of the various SdH signals is different from the original experimental one. We obtain the longitudinal electron cross sections (spin split by a large exchange splitting) to be larger than those for the holes. Because spin-orbit coupling was not included, however, this result must still be considered to be tentative. Second, as noted above for the Fermi-surface volume, all values are larger than experiment. In Ref. 19, we investigated explicitly the effects of the Sc addition and of corrections beyond LDA. The dilution by (nonmagnetic) Sc was found to account well for the reduction of the exchange splitting, but not for the overall size of the Fermi surface. A simple upward shift of the Er-$5d$ (mixed with Sc 3d) band by about 0.4 eV, however, reduces the Fermi surface volume and its various cross sections by the desired amount to agree well with experiment. The origin of this shift is discussed in Sec. V A.

There remain some smaller discrepancies, which were not discussed in Ref. 19. The light-hole (lh) cross section, which was identified by us with a SdH freqeuncy peak at 153 T, is in our calculation found at 281 T, even with the corrected band structure. We note that this is likely to be the result of our neglect of spin-orbit coupling. The latter would shift this band downward and hence reduce its cross section. In fact, in very thin samples where size quantization effects become significant and may shift this level totally below the Fermi level, this signal appears to be absent.[11] Second, a peak in the SdH Fourier transform spectrum was observed at about 600 T.[10,11] This peak was not identified in the earlier work,[9] because it was obscured by the second harmonic signals of the main electron peaks. It was subsequently observed in both magnetoresistance and Hall resistance. Among others, because of its stronger appearance in the Hall resistance, it was identified as being related to holes. This is because the holes and electron conductivities enter in different ways in the longitudinal magnetoresistance and the Hall resistance. The Hall measurement is more sensitive to the holes. Our calculation obtains the heavy-hole peaks at 885 and 925 T. One may again anticipate that spin-orbit coupling will lower the mass of the hh1 band and hence reduce its Fermi-surface cross section. We, thus, think that the 600 T peak is related to the band, which here is called hh1 and which conventionally is called the lh band in semiconductors. Preliminary estimates of the spin-orbit coupling using a Kohn-Luttinger Hamiltonian and a value of 0.3–0.4 eV for the spin-orbit splitting at Γ (i.e., similar to the value in GaAs), indicate that the effect is of the correct order of magnitude to shift the lh peak down to the 600 T region. Likewise, we then expect the heavy-hole peak to shift up. Any change in the total hole Fermi surface volume must be accompanied by a corresponding change in the electron Fermi-surface volume. This means that the identification of the peaks in the 900–1250 T region must still be considered somewhat uncertain. A definitive conclusion on these questions awaits a calculation in which spin-orbit coupling is explicitly included. However, the main point that an LDA correction is required to explain the overall size of the Fermi surface should remain valid.

While the large spin splitting of the electron parts of the Fermi surface are in good agreement with experiment (even without the Er $5d$ band shift correction), the spin splittings of the hole bands are too small to be seen in the SdH measurments. Evidence of their presence, however, was recently

TABLE IV. Cyclotron effective masses of light holes m_l, heavy holes m_{h1}, m_{h2}, and electrons $m_{e,\parallel}, m_{e,\perp}$, which are defined in the text (in units of the free electron mass m_0).

Compound	m_l	m_{h1}	m_{h2}	$m_{e,\parallel}$	$m_{e,\perp}$
GdN	0.20	0.62	0.91	1.32	0.08
GdP	0.12	0.47	0.57	1.57	0.16
GdAs	0.13	0.44	0.47	1.33	0.19
ErN	0.18	0.61	0.87	1.42	0.09
ErP	0.14	0.47	0.54	1.71	0.17
ErAs	0.12	0.46	0.57	1.76	0.17

obtained from resonant tunneling measurements.[20] These results will be discussed elsewhere.[21]

A detailed study of the Fermi surfaces for the other R-V compounds has not yet been made, mainly because of the absence of experimental data for comparison. In addition, the lack of data inhibits us from making empirical adjustments of the overall scale of the Fermi surface volume to compensate for the LDA problem discussed above.

F. Effective masses

The cyclotron effective masses for the carriers are given by[44]

$$m = \frac{\hbar^2}{2\pi} \frac{\partial S_F}{\partial E_F}, \tag{2}$$

where S_F is the area of the extremal cross section of the Fermi surface enclosed by the orbit in the plane normal to the magnetic field. The relevant cross sections of the Fermi surface have already been described in the previous section. We define the corresponding masses as $m(\Gamma XW)$ and $m(WXU)$, respectively. If we model the actual Fermi surface by an ellipsoid of revolution, $m_\perp$ corresponds to $m(WXU)$, and $m_\parallel$ follows from

$$m(\Gamma XW) = (m_\parallel m_\perp)^{1/2}. \tag{3}$$

The value of the cyclotron masses for all the materials are given in the Table IV. We note that the value of $m_\perp = 0.17$ for ErAs is in perfect agreement with the value reported by Allen *et al.*,[8] for $Er_xSc_{1-x}As$ with $x \approx 0.5$. Our previous work[19] shows that the Sc addition only changes this mass by 0.01 to $m_\perp = 0.16$. This mass was also found to be insensitive to the quasiparticle correction of the Er $5d$ band. The longitudinal electron and hole masses were also found to be in fair agreement with the experimental values for $Er_xSc_{1-x}As$, although there are somewhat larger uncertainties for them due to the different possible assignments of the SdH frequencies and the neglect of spin-orbit coupling in our calculations.

Generally speaking, the masses vary only slowly with the energy. Since, as noted above, the quasiparticle corrections lead to a nearly rigid shift of the bands, this implies that the masses are not very sensitive to the corrections. The calculations have verified this.

V. DISCUSSION: CORRECTIONS TO THE LDA

As mentioned in Sec. IV E and discussed in detail in Ref. 19, an upward shift of the Er $5d$ band by about 0.4 eV was found necessary to account for the size of the Fermi surface as given by SdH measurements and carrier concentrations by Hall effect measurements. Here, we discuss two possible origins of this shift. Both are quasiparticle self-energy effects, which are corrections to the LDA. The first kind of self-energy correction that we address is typical of wide bands and is well known to provide the major correction for the underestimate by the LDA of band gaps in semiconductors. We will show that this correction has the correct order of magnitude to account for the empirically determined shift. The second effect that we consider is the interaction of the $4f$ electrons on the states near the Fermi level, i.e., the hybridization terms that we have left out of the Anderson Hamiltonian in our corelike treatment of the $4f$ electrons. We will show that this is expected to lead to negligible corrections.

A. Wide band self-energy corrections

As is well known, the LDA Kohn-Sham eigenvalues do not strictly speaking correspond to quasiparticle excitations. The state of the art for calculating the latter is a so-called GW calculation, which is the first term in Hedin's perturbation series expansion[46] of the self-energy correction terms of the screened Coulomb interaction W and the one-electron Green's function G. While such calculations have been performed for several semiconductors,[47,48] it is quite difficult for materials with d bands. Only one calculation for such a material has been done to our knowledge.[49] A simplified implementation of the GW method was suggested by Bechstedt and del Sole (BDS).[50] It is based on a very simplified tight-binding two band model and provides reasonable agreement with experimental band gaps for many of the A_NB_{8-N} compounds, including some ionic compounds that form in the rocksalt structure, as well as most of the conventional semiconductors, which have the zinc-blende structure.[50] The semimetallic nature of the R-V compounds presents an additional complication for applying the GW method, because one should, in principle, take into account off-diagonal matrix elements of the self-energy operator between valence- and conduction-band states. Neglecting this, the approach of BDS should still provide a meaningful estimate of the expected upward shift of the mainly empty R $5d$-derived conduction band forming the electron pocket at X, with respect to the mainly anion-p derived hole pocket at Γ. The BDS approach is based on evaluating the matrix elements of the difference between the effective Coulomb interaction screened by a model dielectric function for the semiconductor and the Lindhard dielectric function for the free electron gas. The former involves the macroscopic dielectric constant and can be applied to a semimetal if we define an effective dielectric constant $\bar{\epsilon}$ by means of the Penn-Phillips formula[51,52] as

$$\bar{\epsilon} = 1 + (\hbar\omega_p / E_p)^2, \tag{4}$$

where ω_p is the plasma frequency of the valence electrons and E_p is the effective "dielectric" or "Penn" gap. The Penn

TABLE V. Penn gaps (eV), effective dielectric constants, self-energy corrections (eV), LSDA and LDA "band gaps" (eV), and estimated "band gaps" (eV), with self-energy corrections included.

Compound	E_p	$\bar{\epsilon}$	ΔE_g	$E_g^{F,\mathrm{LSDA}}$	$E_g^{P,\mathrm{LDA}}$	$E_g^{F,\mathrm{est}}$	$E_g^{P,\mathrm{est}}$
GdN	3.72	26.5	0.28	−0.49	−0.18	−0.21	0.10
GdP	3.22	23.9	0.27	−1.50	−1.04	−1.23	−0.77
GdAs	3.18	22.8	0.28	−1.66	−1.19	−1.37	−0.91
ErN	4.22	22.9	0.33	−0.26	−0.15	0.07	0.18
ErP	3.39	22.9	0.29	−1.61	−1.53	−1.32	−1.24
ErAs	3.35	22.1	0.22	−1.65	−1.63	−1.36	−1.41

gap may be estimated as the gap between valence and conduction bands at the Baldereschi point[53,54] $\mathbf{k}_B=(0.622,0.295,0)2\pi/a$. The quantity $\bar{\epsilon}$ is certainly meaningful for narrow-gap semiconductors such as Ge and such as the ErN considered here, which have a semimetallic band structure in LDA, but become a semiconductor when the gap correction is applied. It still retains an approximate validity even for true semimetals,[52] because their optical response is still dominated by a peak at the Penn gap. We can, thus, use it for an estimate of the gap correction ΔE_g, which in the BDS approach[50] is given by

$$\Delta_g=\frac{q_{\mathrm{TF}}}{\bar{\epsilon}}(1+7.62q_{\mathrm{TF}}r_{\mathrm{eff}})^{-1}. \tag{5}$$

Here, q_{TF}, is the Thomas-Fermi wave vector and

$$r_{\mathrm{eff}}=\left[(1-\alpha_p)\frac{r_A}{2}+(1+\alpha_p)\frac{r_B}{2}\right] \tag{6}$$

is an effective radius, given in terms of the polarity of the bonds α_p (which is obtained from atomic energy levels as in Harrison's universal tight-binding approach[55]) and effective radii of cation and anion Slater orbitals given as $r_{A/B}=(a/4\pi)(1.7\mp 0.05|Z_A-Z_B|)$.

The quantities E_p, $\bar{\epsilon}$, and ΔE_g are summarized in Table V. One can see that for all compounds considered $\Delta E_g\sim 0.3$ eV, which is rather small compared to that found in most semiconductors. The main reason for this is the large value of $\bar{\epsilon}$.

One can define the "band gap," E_g, of *R-V* compounds as the difference between the top of the "valence band" Γ_{15} and the bottom of the "conduction band" X_3 in the paramagnetic phase and as the difference between the spin-down energy $X_{3\downarrow}$ and the spin-up energy $\Gamma_{15\uparrow}$ in the ferromagnetic phase. In the nitrides, X_3 is the X state closest to E_F, while in the phosphides and arsenides, it lies below the doubly degenerate X_5 state due to the crossing of the Δ_5 and Δ_2' bands.

Our calculated values for the gaps with and without spin polarization and with and without the corrections are listed in Table V. We first note that the arsenides and phosphides remain semimetals even with the correction, in agreement with experiment. The self-energy shift of the conduction band must be accompanied by a corresponding shift in the valence band both measured from the Fermi level in order to maintain an equal electron and hole concentration, as is required by the present Fermi-surface topology. These shifts significantly decrease the concentration of electrons and holes. From the magnitude of the shift, we estimate that the concentrations may generally decrease by a factor two to three. For $Er_xSc_{1-x}As$ and ErAs, where a comparison to experiment is possible, we found[19] that a shift of 0.4 eV accounts for the observed carrier concentrations of $n_{e,h}\approx 3\times 10^{20}$ cm^{-3}. The estimated uncertainty in the BDS approach is of order 0.2 eV. The Er $5d$ band shift (0.22 eV) calculated from the BDS approach is thus of the right order of magnitude. The *GW* self-energy correction is thus at least a plausible cause for the required shift.

Next, we note that the corrections are rather similar in the whole series of compounds under study. We, thus, may expect similar shifts of order 0.2–0.4 eV, for the band gaps of the other compounds. While for phosphides and arsenides the estimated self-energy corrections give rise only to quantitative changes (mostly a reduction of the carrier concentration), for the nitrides they may lead to qualitative changes of the electronic structure. Indeed, the corrections predict ErN to be a semiconductor both in the paramagnetic and the ferromagnetic phase (see Table V). GdN reveals even more interesting features — it would be a semiconductor in the paramagnetic phase and a semimetal in the ferromagnetic phase. These calculations thus predict a metal-insulator phase transition in GdN as a function of external magnetic field or temperature. Furthermore, the nature of this transition is rather unusual: whereas many systems open a gap when the spins are polarized, the opposite effect is predicted here. As mentioned in the introduction, we should also keep in mind that very near the zero gap crossing, an electron-hole liquid may spontaneously form.[17] The fact that in GdN one might tune through this transition by simply changing the magnetic field is quite appealing. In addition, the resulting electron-hole liquid would have the unique property of involving electrons of only one spin and holes of the opposite spin.

Because of the rather large uncertainties on our estimates of the self-energy corrections, these conclusions are still somewhat tentative. A more detailed theory should take into account quasiparticle corrections to the self-energy and effects of spin disorder on an equal footing. Nevertheless, it appears worthwile to try to confirm these predictions by experiment because of the possibly interesting phenomena associated with such an unusual metal-insulator transition.

B. Hybridization with 4*f* bands

A second possible cause for the upward shift in the Er $5d$ band near the Fermi level that we need to consider is the interaction of the $5d$ band with the $4f$ states that we have neglected by the artifice of handling the latter as a core state. As discussed in Sec. II, the $4f$ bands are expected to give

rise to narrow bands both below and above the Fermi level. To assess its importance, we first study a simple analytically solvable tight-binding model, which provides us with explicit relations between the desired $5d$ band shift and its model parameters such as bandwidths, effective Coulomb interaction, and the d-f energy level difference. We can then by analogy apply these simple relations appropriately adapted to the present system. We emphasize that the simple model from which the relations are derived is not meant to provide a realistic description of the rare-earth compounds.

For simplicity, we first consider a simple cubic model in which d orbitals and f orbitals are replaced by nondegenerate s-like orbitals, so that we have only two orbitals per R site. The Anderson-impurity Hamiltonian for this system is

$$\begin{aligned}\hat{H}=&\sum_{i\sigma}\ \epsilon_d d^{\dagger}_{i\sigma}d_{i\sigma}+\sum_{i\sigma}\ \epsilon_f f^{\dagger}_{i\sigma}f_{i\sigma}\\&+V_{df}\sum_{\langle ij\rangle}\ \sum_{\sigma}\ (d^{\dagger}_{i\sigma}f_{j\sigma}+f^{\dagger}_{j\sigma}d_{i\sigma})\\&+V_{dd}\sum_{\langle ij\rangle}\ \sum_{\sigma}\ (d^{\dagger}_{i\sigma}d_{j\sigma}+d^{\dagger}_{j\sigma}d_{i\sigma})\\&+\frac{U}{2}\sum_{i\sigma}\ (\hat{n}_{fi\sigma}\hat{n}_{fi-\sigma}-n_f\hat{n}_{fi\sigma}),\end{aligned}\tag{7}$$

with σ being the spin index. Here, only on-site Coulomb terms are included and then only for the localized f electrons, since the d orbitals are meant to represent any broadband for which an effective one-electron model is appropriate. Also, only d-d and d-f hopping terms are included. The average number of f electrons per site n_f appears in the last term and is a constant. This term avoids double counting of interactions already included in the one-electron terms. We will focus on the half-filled f-band case $n_f=1$. The above simple model is almost directly applicable to GdAs, which has indeed a half-filled f shell — apart from the obvious complications of dealing with the degeneracies of f and d states.

In this model, when we take $U=0$ and we assume that the f level and d band are in separate energy regions so that we can apply downfolding (or second order perturbation theory) for the interaction of the f- and d orbitals, we obtain a d band width

$$W_d=2NV_{dd}+V_{df}^2N^2/(\epsilon_d-\epsilon_f),\tag{8}$$

with $N=6$ the number of nearest neighbors. Clearly, the first term comes from the direct d-d hopping, while the second comes from the indirect interactions via the f orbital. Similarly, the f level also broadens into a band given by

$$E_f=\epsilon_f+\frac{[2V_{df}\Sigma_{\alpha}\cos(k_{\alpha}a)]^2}{\epsilon_d+2V_{dd}\Sigma_{\alpha}\cos(k_{\alpha}a)-\epsilon_f},\tag{9}$$

with width

$$W_f=(NV_{df})^2/(\epsilon_d\pm NV_{dd}-\epsilon_f),\tag{10}$$

and where the $+(-)$ prevails if $V_{dd}>0$ (<0).

When the U term is added in the mean field approximation (spcified by $\hat{n}_{fi\sigma}\hat{n}_{fi-\sigma}=\hat{n}_{fi\sigma}\langle n_{fi-\sigma}\rangle+\hat{n}_{fi-\sigma}\langle n_{fi\sigma}\rangle$), the majority spin $f\downarrow$ level is shifted down by $U/2$, while the minority spin $f\uparrow$ level is pushed up by $U/2$: $\epsilon_{f\uparrow(\downarrow)}=\epsilon_f\pm U/2$. If we neglect V_{dd} in the denominator in Eq. (10), which is legitimate if the d band and f band are well separated, we see that $W_f\propto V_{df}^2/(\epsilon_d-\epsilon_f)$, while the interaction effects on the d band, due to the interaction with the f-levels split by U, is given by $V_{df}^2/(\epsilon_f\pm U/2-\epsilon_d)$. Thus, if U is comparable in magnitude with $|\epsilon_d-\epsilon_f|$, we can estimate the f-level hybridization effects to be about half the width of the f band. If $U\gg|\epsilon_d-\epsilon_f|$, then the hybridization effect is of the order $2V_{df}^2/U$.

From the test calculations of Sec. III, we can place an upper limit of 0.2 eV on W_f, since the bandwidth of the actual $4f$ band includes both hopping between $4f$ states and hybridization with the other bands. The effective U can be estimated from a combination of photoemission and inverse photoemission data on pure rare-earth metals.[32] For Gd, the occupied $4f$ states form a narrow multiplet at 8 eV below the Fermi level, while the unoccupied states lie 4 eV above the Fermi level (also in a narrow multiplet). In Er, there are several occupied multiplet states spread over a considerable range of energy, the highest of which lies about 4 eV below the Fermi level, while the lowest unoccupied multiplet lies about 2 eV above the Fermi level. The $|\epsilon_d-\epsilon_f|$ value can be estimated, from the center-of-the-band potential parameters C_l in our LMTO calculations of Sec. III to be about 6–10 eV and is thus comparable to U. We can thus expect interactions of order 0.1 eV. However, in the case of Er, where part of the minority spin $4f$ bands are filled and part are empty, there will be a significant cancellation between upward shifts by interactions with the occupied lower $4f$ states and a downward shift from interactions with the empty higher lying $4f$ states. We thus expect that the net effect on the bands near the Fermi level will be smaller than 0.1 eV. One might perhaps also expect a small reduction of the spin splitting, because the majority spin electrons only will suffer upward shifts from the $4f$ interactions, while the minority spin electron band is expected to suffer the largest interaction from the closest lying $4f$ band, which is above it.

We can also estimate directly the magnitude of the V_{df} hopping integrals using the LMTO expression $\sqrt{\Delta_f}S_{df}\sqrt{\Delta_d}$, where $\Delta_{d,f}$ are potential parameters and S_{df} are structure constants. For example, $S_{df\sigma}=10\sqrt{35}(w/d)^6$ in the unscreened representation, our calculated potential parameters $\Delta_{5d}\approx 1$ eV, $\Delta_{4f}\approx 0.04$ eV, which gives $V_{df\sigma}\approx 0.02$ eV. Taking into account a degeneracy factor for f orbitals of 7, the net shift of a single d band by its interaction with the f's is expected to be of order $7(NV_{df})^2/(\epsilon_f-\epsilon_d\pm U/2)$, which again is expected to be slightly below 0.1 eV. This is consistent with the above estimates, which were based on the test calculations of Sec. III, which in some sense contain the hybridization and structural aspects more realistically.

As a further confirmation, we performed calculations for GdAs starting from the Gd $4f$ band treatment of Sec. III, in which we artificially shifted the minority Gd $4f$ potential parameters up by an arbitrary $U\uparrow$ shift and the majority Gd $4f$ potential parameters down by $U\downarrow$, while keeping all re-

maining potential parameters frozen. When the $4f$'s were shifted by U's obtained from experiment as discussed above, we found that their effect on the Gd $5d$ band near X became negligible. However, there still was a substantial effect on the As $4p$-like hole bands near Γ. In ErAs, a similar treatment faces the problem that the spin-down $4f$ band is still partially occupied. The crystal field splitting of the f states leads to a three-fold state followed by a singlet and another three-fold state. One should, thus, occupy the lower triplet and the singlet and empty the higher triplet, which would thus be placed above the Fermi level by the U interaction. We have not yet pursued this possibility. By placing the complete set of spin-down states either above or below the Fermi level with arbitrary U shifts, we found that opposite shifts of order 0.1 eV were introduced on the Er $5d$ bands near the Fermi level, consistent with the above estimates.

Since these U shifts are rather arbitrary, we do not show these results explicitly here. They only serve to confirm our order of magnitude estimates of the $4f$ effects. A second problem with these frozen potential parameter calculations is that the remaining potential parameters are affected by their interaction with the $4f$'s through the latter's effect on the self-consistent potential. In fact, the latter was calculated with unshifted LSDA treated $4f$'s. We found that this gave generally worse agreement with experiment for the Fermi-surface parameters. This indicates that if we wish to treat $4f$'s as bands in an "LDA+U" treatment, a self-consistent treatment of the potentials in the presence of the U-shifted $4f$'s will be essential.

Finally, we found that in these frozen potential parameter calculations for ErAs with shifted $4f$ bands, the overestimation of the Fermi-surface volume by a factor 2–3 persisted. We, thus, conclude that although a more elaborate treatment of $4f$ states (e.g., based on "LDA+U") would be of interest, $4f$ interaction effects cannot be the main origin of the large overestimate of the Fermi-surface volume by the LDA.

VI. CONCLUSIONS

We have presented results of first-principles local spin-density functional calculations of the electronic band structures, equilibrium lattice constants, cohesive energies, bulk moduli, and magnetic moments for the rare-earth pnictides with rocksalt structure and chemical formula R-V, where R=Gd, Er and V=N, P, As. These results were obtained using the linear-muffin-tin-orbital method in the atomic sphere approximation and treating the localized $4f$ electrons as atomic boundary insensitive corelike electrons.

We conclude this treatment of the $4f$ electrons is quite satisfactory for most purposes not directly involving the $4f$ states. This treatment was found to provide lattice constants in good agreement with experiment showing that the $4f$'s are not significantly involved in the bonding in these materials and that their charge density is well represented. It accounts well for the major features of the electronic structure and magnetic properties of this family of materials. In particular, it leads to a semimetallic band structure (bordering on a transition to semiconductors for the nitrides), while a straightforward band treatment of the $4f$ states does not. Furthermore, the maximum electron spin alignment of the localized $4f$ electrons provides a natural explanation for the existence of well established local moments, which in turn induces exchange splittings in the valence bands in the presence of an external magnetic field or in the low temperature (anti-) ferromagnetic phases. This induced itinerant magnetism although small leads to observable effects in magnetotransport. The persistence of such moments also explains the small energy difference between the nonmagnetic and magnetic phases (because the latter is almost entirely due to the small induced moments), which is consistent with the small Néel temperatures observed in ErAs and ErP. Furthermore, we showed that interaction effects between the actual $4f$ multiplets and the bands in the neighborhood of the Fermi level are expected to be small. Although we have in the present work not attempted to directly determine the actual positions of the $4f$-derived bands with respect to the bands, we anticipate that this can be achieved by means of Slater's transition state rule and expect them to be similar to those in the corresponding pure rare-earth metals.

Our calculations provide several predictions of presently unknown properties of these materials. These include the bulk moduli and induced magnetic moments, as well as band-structure dispersions, band gaps, effective masses, and exchange splittings. For ErAs, the only material in this family that has been studied experimentally to some extent, we obtain good agreement for most of the band-structure related properties, as determined from magnetotransport measurements. This is the case for the overall topology of the Fermi surface, the exchange splittings and the effective masses. We reviewed our previous detailed study[19] of the magnetotransport properties in $Er_xSc_{1-x}As$ and augmented it in view of recent additional measurements. We concluded that inclusion of the spin-orbit coupling is likely to explain the remaining discrepancies. The only exception to the good agreement is the overall size of the Fermi surface, as determined by Shubnikov–de Haas oscillations and the carrier concentration obtained from Hall effect measurements. In fact, we found that our LDA calculations give an overestimate of the Fermi-surface volume by about a factor of three. This discrepancy, however, could be eliminated by a simple rigid band shift of the Er $5d$ band by only 0.4 eV. A shift of this magnitude can be expected to arise from quasiparticle self-energy corrections of the same type that affect band gaps in semiconductors. This was shown by explicitly estimating such corrections within a simple model. While, unfortunately, this model is too crude to allow an accurate determination, it does yield roughly the correct shift for for ErAs. Furthermore, since the gap corrections were predicted by the simple model to be rather constant throughout the series of materials investigated, we can with some confidence expect corrections for the other materials of roughly the same magnitude as for ErAs. This allows us, for example, to predict that ErN and Gd are narrow gap semiconductors in their paramagnetic phases.

However, our calculations predict that the induced exchange splittings in GdN are sufficiently large that the gap would disappear in the ferromagnetic phase, because the minority spin bands would still overlap in a semimetallic fashion. This is due first of all to the smallness of the gaps in the nonmagnetic case and second to the large magnetic effects induced by the half-filled Gd $4f$ band, which are further

enhanced (relative to the other Gd pnicitides) by the more ionic nature of the nitrides. Another interesting prediction of our calculations for GdN is that the semimetallic overlap of the Gd $5d$ bands near X and As $4p$-derived bands near Γ only occurs for the minority spin bands. This is true even in our LSDA calculation and remains the case after the gap correction is applied as long as the gap correction remains smaller than the negative LSDA gap of the minority spin band. This situation is of interest as it would lead to carriers of only one spin direction. This may be of interest for experiments in which one would like to inject carriers of a given spin polarization into a semiconductor or two-dimensional (2D) electron gas (provided that a 2D electron gas could be formed at an interface with GdN). Further interest in this system arises from the fact that this semimetal-semiconductor transition may be accompanied by the formation of an electron-hole liquid near the zero gap crossing. An electron-hole liquid, which, furthermore, may have unique properties, due the spin polarization of its components and, the density of which might be changed by the application of an external magnetic field. Although these conclusions about GdN are still somewhat tentative, because of the limited accuracy of our estimate of the band-gap self-energy correction, we think this phenomenon of a magnetic field induced semiconductor to metal transition is sufficiently different that we find it worthwile drawing attention to it. Hopefully an experimental verification will be undertaken. Finally, we note that even if in pure GdN the gap correction turns out to be large enough to eliminate the effect, one could expect that the desired situation would hold in a suitable GdP_xN_{1-x} alloy, because one expects alloying would allow one to tune the gap to the desired value in relation to the spin splitting.

We conclude that the electronic and magnetic properties of the rare-earth pnictides are quite interesting, because of their unusual combination of a semimetallic or semiconducting character with the magnetism induced by the strong coupling to the $4f$ localized moments. In particular, this implies that the Fermi surface may be affected efficiently by a moderate external magnetic field.

ACKNOWLEDGMENTS

This work was supported by AFOSR Grant No. F49620-95-1-0043 and ONR Grant No. N00014-93-10425. One of us (A.G.P.) acknowledges the partial support of the National Science Foundation under Grant No. OSR-9108773 and of the South Dakota Future Fund.

*Present address.

[1] F. Hulliger, in *Handbook on the Physics and Chemistry of Rare Earths*, edited by K. A. Gshneidner and L. Eyring (North-Holland, Amsterdam, 1979), Vol. 4, p. 153.

[2] H. R. Child, M. K. Wilkinson, J. W. Cable, W. C. Koehler, and E. O. Wollan, Phys. Rev. **131**, 922 (1963).

[3] N. Dai, H. Luo, F. C. Zhang, N. Samarth, M. Dobrowolska, and J. K. Furdyna, Phys. Rev. Lett. **67**, 3824 (1991).

[4] C. J. Palmstrøm, N. Tabatabaie, and S. J. Allen, Jr., Appl. Phys. Lett. **53**, 2608 (1988).

[5] S. J. Allen, D. Brehmer, and C.J. Palmstrøm, in *Rare Earth Doped Semiconductors*, edited by S. Pomrenke, P. B. Klein, and D. W. Langer, MRS Symposia Proceedings No. 301 (Materials Research Society, Pittsburgh, 1993), p. 307.

[6] A. Guivarc'h, Y. Ballini, M. Minier, B. Guenais, G. Dupas, G. Ropars, and A. Regreny, J. Appl. Phys. **73**, 8221 (1993); A. Guivarc'h, Y. Ballini, P. Auvray, J. Caulet, M. Miner, G. Dupas, and G. Ropars, *ibid.* **74**, 6632 (1993); A. Guivarc'h, B. Guenais, Y. Ballini, P. Auvrau, J. Caulet, M. Minier, G. Dupas, G. Ropars, R. Guérin, and S. Députier, J. Cryst. Growth **127**, 638 (1993).

[7] A. Le Corre, B. Guenais, A. Guivarc'h, D. LeCrosnier, J. Caulet, M. Minier, G. Ropars, P. A. Badoz, and J. Y. Duboz, J. Cryst. Growth **105**, 234 (1990); A. Le Corre, J. Caulet, and A. Guivarc'h, Appl. Phys. Lett. **55**, 2298 (1989).

[8] S. J. Allen, Jr., N. Tabatabaie, C. J. Palmstrøm, G. W. Hull, T. Sands, F. DeRosa, and H. L. Gilchrist, Phys. Rev. Lett. **62**, 2309 (1989); S. J. Allen, Jr., F. DeRosa, C. J. Palmstrøm, and A. Zrenner, Phys. Rev. B **43**, 9599 (1991).

[9] R. Bogaerts, L. Van Bockstal, F. Herlach, F. M. Peeters, F. DeRosa, C. J. Palmstrøm, and S. J. Allen, Jr., Physica B **177**, 425 (1992).

[10] R. Bogaerts, L. Van Bockstal, F. Herlach, F. M. Peeters, F. DeRosa, C. J. Palmstrøm, and S. J. Allen, Jr., Physica B **184**, 2320 (1993).

[11] R. Bogaerts, Ph.D. thesis, Katholieke Universiteit Leuven, 1994.

[12] A. Hasegawa and A. Yanase, J. Phys. Soc. Jpn. **42**, 492 (1977).

[13] A. I. Liechtenstein, V. P. Antropov, and B. N. Harmon, Phys. Rev. B **49**, 10 770 (1994).

[14] S. P. Lim and B. R. Cooper, Bull. Am. Phys. Soc. **39**, 394 (1994).

[15] A. Hasegawa, J. Phys. Soc. Jpn. **54**, 677 (1985).

[16] G. Travaglini, F. Marabelli, R. Monnier, E. Kaldis, and P. Wachter, Phys. Rev. B **34**, 3876 (1986).

[17] R. Monnier, J. Rhyner, T. M. Rice, and D. D. Koelling, Phys. Rev. B **31**, 5554 (1985).

[18] Jian-Bai Xia, Shang-Fen Ren, and Yia-Chung Chang, Phys. Rev. B **43**, 1692 (1991).

[19] A. G. Petukhov, W. R. L. Lambrecht, and B. Segall, Phys. Rev. B **50**, 7800 (1994).

[20] Kai Zhang, D. E. Brehmer, S. J. Allen, Jr., and C. H. Palmstrøm (unpublished); D. E. Brehmer, Kai Zhang, Ch. J. Schwarz, S.-P. Chau, S. J. Allen, J. P. Ibbetson, J. P. Zhang, C. J. Palmstrøm, and B. Wilkens (unpublished).

[21] A. G. Petukhov, W. R. L. Lambrecht, and B. Segall, Phys. Rev. B (to be published).

[22] A. G. Petukhov, W. R. L. Lambrecht, and B. Segall, in *Advanced Metallization for Devices and Circuits—Science, Technology, and Manufacturability*, edited by S. P. Murarka, A. Katz, K. N. Tu, and K. Maex, MRS Symposia Proceedings No. 337 (Materials Research Society, Pittsburgh, 1994), p. 583.

[23] P. Hohenberg and W. Kohn, Phys. Rev. **136**, B864 (1964); W. Kohn and L. J. Sham, *ibid.* **140**, A1133 (1965).

[24] U. von Barth and L. Hedin, J. Phys. C **5**, 1629 (1972).

[25] O. K. Andersen, O. Jepsen, and M. Šob, in *Electronic Band Structure and its Applications*, edited by M. Yussouff (Springer, Heidelberg, 1987), p. 1.

[26] Originally introduced by D. Glötzel and O. K. Andersen (unpublished); see Ref. 25 for a discussion.

[27] D. Glötzel, B. Segall, and O. K. Andersen, Solid State Commun. **36**, 403 (1980).

[28] O. Jepsen and O. K. Andersen, Solid State Commun. **9**, 1763

(1971); P. E. Blöchl, O. Jepsen, and O. K. Andersen, Phys. Rev. B **49**, 16 223 (1994).
[29] P. W. Anderson Phys. Rev. **124**, 41 (1961).
[30] V. I. Anisimov and O. Gunnarsson, Phys. Rev. B **43**, 7570 (1991).
[31] J. C. Slater, *The Self-Consistent Field for Molecules and Solids* (McGraw-Hill, New York, 1974), Vol. 4, p. 35.
[32] J. K. Lang, Y. Baer, and P. A. Cox, J. Phys. F **11**, 121 (1981).
[33] J. F. Herbst, D. N. Lowy, and R. E. Watson, Phys. Rev. B **6**, 1913 (1972).
[34] Tôru Moriya, J. Magn. Magn. Mater. **14**, 1 (1979).
[35] M. S. S. Brooks, L. Nordström, and B. Johansson, J. Phys. Condens. Matter **3**, 2357 (1991).
[36] W. M. Temmerman and P. A. Sterne, J. Phys. C **2**, 5529 (1990).
[37] D. J. Singh, Phys. Rev. B **44**, 7451 (1991).
[38] M. Heinemann and W. M. Temmerman, Phys. Rev. B **49**, 4348 (1994).
[39] R. Ahuja, S. Auluck, B. Johansson, and M. S. S. Brooks, Phys. Rev. B **50**, 5147 (1994).
[40] P. H. Dederichs, S. Blügel, R. Zeller, and H. Akai, Phys. Rev. Lett. **53**, 2512 (1984).
[41] V. I. Anisimov, J. Zaanen, and O. K. Andersen, Phys. Rev. B **44**, 943 (1991); V. I. Anisimov, I. V. Solovyev, M. A. Korotin, M. T. Czyżyk, and G. A. Sawatzky, *ibid.* **48**, 16 929 (1993).
[42] D. M. Bylander and L. Kleinman, Phys. Rev. B **49**, 1608 (1994).
[43] J. H. Rose, J. R. Smith, F. Guinea, and J. Ferrante, Phys. Rev. B **29**, 2963 (1984).
[44] J. M. Ziman, *Principles of the Theory of Solids* (Cambridge University Press, Cambridge, England, 1972), Chap. 9.
[45] J. F. Herbst, D. N. Lowy, and R. E. Watson, Phys. Rev. B **6**, 1913 (1972).
[46] L. Hedin, Phys. Rev. **139**, A796 (1965); L. Hedin and S. Lundqvist, in *Solid State Physics: Advances in Research and Applications*, edited by F. Seitz, D. Turnbull, and H. Ehrenreich (Academic, New York, 1969), Vol. 23, p. 1.
[47] M. Hybertsen and S. G. Louie, Phys. Rev. B **34**, 5390 (1986)
[48] R. W. Godby, M. Schlüter, and L. J. Sham, Phys. Rev. B **37**, 10 159 (1988).
[49] F. Aryasetiawan, Phys. Rev. B **46**, 13 051 (1992).
[50] F. Bechstedt and R. del Sole, Phys. Rev. B **38**, 7710 (1988).
[51] D. Penn, Phys. Rev. **128**, 2093 (1962).
[52] J. C. Phillips, *Bonds and Bands in Semiconductors* (Academic, New York, 1973).
[53] A. Baldereschi, Phys. Rev. B **7**, 5212 (1973).
[54] M. Cardona and N. E. Christensen, Phys. Rev. B **35**, 6182 (1987).
[55] W. A. Harrison, *Electronic Structure and Properties of Solids* (Freeman, San Francisco, 1980).